ATP-binding cassette transporters restrict drug delivery and efficacy against brain tumors even when blood-brain barrier integrity is lost

Gooijer, M.C. de; Kemper, E.M.; Buil, L.C.M.; Citirikkaya, C.H.; Buckle, T.; Beijnen, J.H.; Tellingen, O. van

Cell Reports
Medicine

Article

ATP-binding cassette transporters restrict drug delivery and efficacy against brain tumors even when blood-brain barrier integrity is lost

Graphical Abstract

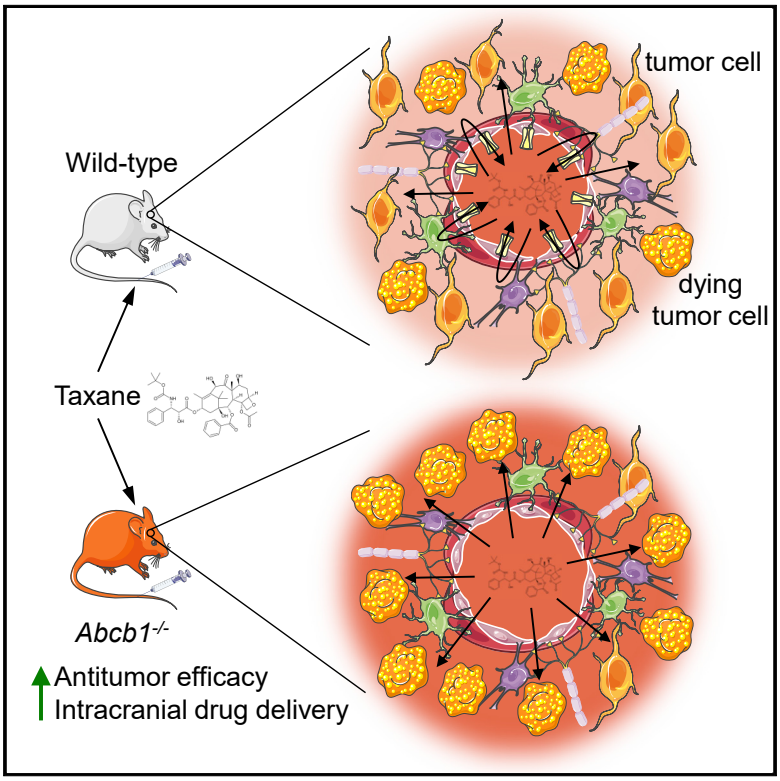

Authors

Mark C. de Gooijer, E. Marleen Kemper, Levi C.M. Buil, Ceren H. Çitirikkaya, Tessa Buckle, Jos H. Beijnen, Olaf van Tellingen

Correspondence

o.v.tellingen@nki.nl

In Brief

Whether a compromised blood-brain barrier hinders the drug treatment of intracranial tumors remains controversial. de Gooijer et al. determine how drug transporters affect the efficacy of docetaxel against several intracranial tumor models with various levels of blood-brain barrier integrity and show that ABC transporters can restrict drug efficacy even when tumor vessels are leaky.

Highlights

- Blood-brain barrier integrity in brain tumor models varies from intact to absent
- Brain tumor vessels express drug efflux transporters
- Drug transporters can impede drug entry and efficacy, even in leaky tumors
- Low-affinity ABC transporter drugs are favored candidates for treating brain tumors

de Gooijer et al., 2021, Cell Reports Medicine 2, 100184
January 19, 2021
https://doi.org/10.1016/j.xcrm.2020.100184

CellPress

Cell Reports Medicine

CellPress
OPEN ACCESS

Article

ATP-binding cassette transporters restrict drug delivery and efficacy against brain tumors even when blood-brain barrier integrity is lost

Mark C. de Gooijer,[1,2] E. Marleen Kemper,[3] Levi C.M. Buil,[1,2] Ceren H. Çitirikkaya,[1,2] Tessa Buckle,[4] Jos H. Beijnen,[1,5,6] and Olaf van Tellingen[1,2,7,*]

[1]Division of Pharmacology, the Netherlands Cancer Institute, Amsterdam, the Netherlands
[2]Mouse Cancer Clinic, the Netherlands Cancer Institute, Amsterdam, the Netherlands
[3]Department of Hospital Pharmacy, Academic Medical Center, Amsterdam, the Netherlands
[4]Department of Radiology, Leiden University Medical Center, Leiden, the Netherlands
[5]Department of Pharmacy and Pharmacology, the Netherlands Cancer Institute, Amsterdam, the Netherlands
[6]Division of Pharmacoepidemiology and Clinical Pharmacology, Department of Pharmaceutical Sciences, Faculty of Science, Utrecht University, Utrecht, the Netherlands
[7]Lead contact
*Correspondence: o.v.tellingen@nki.nl
https://doi.org/10.1016/j.xcrm.2020.100184

SUMMARY

The impact of a compromised blood-brain barrier (BBB) on the drug treatment of intracranial tumors remains controversial. We characterize the BBB integrity in several intracranial tumor models using magnetic resonance imaging, fluorescent dyes, and autoradiography and determine the distribution and efficacy of docetaxel in brain tumors grafted in Abcb1-proficient and Abcb1-deficient mice. Leakiness of the tumor vasculature varies from extensive to absent. Regardless of the extent of leakiness, tumor blood vessels express ATP-binding cassette transporters (Abcb1 and Abcg2). A leaky vasculature results in higher docetaxel tumor levels compared to normal brain. Nevertheless, Abcb1 can reduce drug distribution and efficacy even in leaky models. Thus, BBB leakiness does not ensure the unimpeded access of ATP-binding cassette transporter substrate drugs. Therapeutic responses may be observed, but the full potential of such therapeutics may still be attenuated. Consequently, BBB-penetrable drugs with little to no affinity for efflux transporters are preferred for the treatment of intracranial tumors.

INTRODUCTION

High-grade gliomas, and in particular glioblastoma (GBM), are the most common primary malignant brain tumors in adults and invariably lethal. The established treatment consists of surgical resection to a maximum safe extent, followed by external beam radiotherapy and temozolomide chemotherapy.[1] Because of the widespread infiltration of tumor cells into the surrounding brain structures, complete surgical resection of malignant glioma is impossible. Therefore, the challenge of improving GBM therapy is to design therapies that are able to track and kill those residual tumor cells left within the brain following surgery.[2] So far, however, no systemic chemotherapeutic drugs other than temozolomide have shown significant efficacy in the treatment of malignant gliomas, neither as monotherapy or in combination strategies. A likely contributing factor to the low efficacy of chemotherapy is the presence of the blood-brain barrier (BBB), which limits the brain penetration of many anticancer drugs.[3] Improving drug delivery into the brain will therefore be an important first step when considering the chemotherapeutic treatment of GBM.[4] The BBB is physically formed by the endothelial cells of the brain. The typical BBB features of the endothelium are induced by intimate contact with astrocytes and/or pericytes.[5,6] Brain endothelial cells lack fenestrations and are closely linked by tight junctions. Besides these passive constraints, active efflux of compounds from the brain by the ATP-binding cassette (ABC) transporters P-glycoprotein (P-gp; ABCB1), breast cancer resistance protein (BCRP; ABCG2), and multidrug resistance-associated protein 4 (MRP4; ABCC4) has been well established.[5,7]

GBM as well as brain metastases are known to disrupt BBB integrity as is visualized by gadolinium contrast-enhanced magnetic resonance imaging (MRI).[8,9] Penetration of this small molecule contrast agent to the tumor fuels the notion that other small-molecule drugs may have similar good access to the tumor. Notably, however, disruption of the BBB in GBM occurs mainly in the core of the tumor, where microvascular proliferation results in newly formed leaky blood vessels. In contrast, the BBB is more intact in the peripheral zones and brain adjacent to tumor areas where numerous infiltrating tumor cells reside that are typically left behind following surgery.[2,4] Heterogeneity in BBB disruption is also evident in brain metastases.[10] There are several examples in which a tumor growing outside the brain

responds better to therapies compared to the same tumor growing intracranially.[11,12] It is therefore very likely that the BBB remains a hurdle, limiting the entry of therapeutics into substantial areas of GBM tumor tissue in patients.

Paclitaxel and docetaxel are efficacious in the treatment of patients with various extracranial malignancies such as ovary, breast, and lung cancer,[13] but not against malignant gliomas.[14,15] In general, cell lines derived from malignant glioma are equally sensitive to low nanomolar concentrations of paclitaxel and docetaxel as cell lines of other origin, showing that malignant glioma cells are not intrinsically resistant.[16,17] Paclitaxel and docetaxel are substrates of the drug efflux pump P-gp, and the brain penetration of docetaxel and paclitaxel in P-gp knockout (KO) mice is >5- to 10-fold higher than in wild-type (WT) mice.[18,19] We have characterized the BBB in a series of intracranial xenograft tumor models, including a serum-free cultured glioma stem cell model, which encompass various degrees of BBB leakiness. By using recipient nude mice that are proficient or deficient in P-gp in combination with a P-gp substrate chemotherapeutic drug, we were able to determine the potential impact of drug transporters in leaky and non-leaky tumor areas on drug distribution and efficacy. Importantly, our work shows that ABC transporters in the tumor vasculature are functionally important and protect areas of tumors that are evidently leaky. This result emphasizes the need to use BBB-penetrable drugs when treating intracranial tumors.

RESULTS

Characterization of the leakiness of intracranial tumor models

To assess the impact of the leakiness of the tumor vasculature on the efficacy of drug treatment, we characterized a series of intracranial tumor models by contrast-enhanced MRI with gadolinium as well as by autoradiography with ^{14}C-labeled aminoisobutyrate (AIB) and fluorescence microscopy following the injection of Texas Red (TxRed). We started with four models for our further study, since these recapitulate the spectrum from minimally to highly leaky tumors (Figures 1 and S1).

GBM8 is a neurobasal medium-cultured glioblastoma stem cell-like (GSC) line of the proneural subtype. It is a highly invasive tumor that invades the contralateral hemisphere and displays only very minimal contrast enhancement on MRI and only in the more central core of the lesion. Also, the other leakiness markers, AIB and TxRed, indicate minimal to no leakiness. Mel57 is a melanoma cell line that forms more compact tumors, which are not very rich in blood vessels. In addition, this tumor showed some contrast enhancement on MRI, whereas TxRed fluorescence distribution was not detectable. The AIB distribution in these tumors was clearly higher than in the surrounding brain tissue. These results suggest that the BBB in Mel57 is not completely intact, although the extent of leakiness is limited. The same Mel57 cell line transduced with vascular endothelial growth factor (VEGF) resulted in highly vascularized, compact tumors. The MRI showed ring enhancement, whereas the core was less enhanced, indicative of high interstitial pressure in the tumor. Extensive distribution of TxRed surrounding the tumor as well as uptake of AIB was found throughout the tumor, indicating profound leakiness of the BBB in these tumors. U87 is a serum-cultured GBM cell line that forms compact tumors that were also well vascularized. These tumor vessels were leaky, as judged by MRI, TxRed, and AIB distribution.

Notably, all brain tumor lesions uniformly express P-gp and BCRP in the tumor vessels, whether the tumor cells originate from GBM or extracranial tumor types. Of note, immunohistochemical staining of P-gp on mouse tissue slides is not straightforward. We have tested many antibodies over the last several years without much success. In most cases, there was either no staining of the vessels or the vessels stained nicely, but the same vessel staining was then also found in P-gp KO mice. The current antibody gives some non-specific staining of normal brain cells since this was also found in *Abcb1a/b*$^{-/-}$ mice, but the typical vascular staining of P-gp is only present in mice proficient for P-gp (Figure S2). The antibody for BCRP gives much cleaner results. Note that besides the specific staining of the vessels, there is also a more diffuse staining throughout the normal brain parenchyma in BCRP-proficient mice that is absent in *Abcb1a/b;Abcg2*$^{-/-}$ mice.

P-glycoprotein limits the distribution of docetaxel in brain tumors

Next to the semiquantitative evaluation of leakiness of the BBB in tumors, as described above (see also Figure S1), we conducted a more thorough quantitative assessment by determining the distribution of docetaxel in our panel of intracranial tumor models as well as in ipsilateral (right) and contralateral (left) brain hemispheres and cerebellum. Tumor cells were injected into the striatum in the right hemisphere and were allowed to grow to a size that allowed visual recognition and isolation of sufficient material for analysis. U87 tumors form solid spherical structures that are easy to isolate without any adjacent normal brain tissue. Mel57-VEGF tumors were soft, but rich in blood vessels and therefore easy to distinguish and isolate from normal brain. Mel57 and GBM8 were more difficult to discern from normal tissue.

The concentration of docetaxel in GBM8 tumor tissue was equal to the concentration in normal brain, and the concentration of the same tumor in *Abcb1a/b*$^{-/-}$ mice was ~5-fold higher (Figure 2). This result is in line with the findings by MRI, AIB, and TxRed that show that GBM8 tumors have an almost intact BBB. However, in Mel57 tumors that also appear to have a non-leaky BBB, the concentration of docetaxel was ~5-fold higher than in the normal brain of the same WT mice. Mel57 tumors in *Abcb1a/b*$^{-/-}$ mice accumulated ~2.5-fold more docetaxel than tumors in WT mice. This result demonstrates that docetaxel is able to accumulate into the tumor, but that despite this leakiness, P-gp is still capable of reducing the accumulation in the tumor. A much higher concentration of docetaxel was observed in Mel57VEGF tumors, and the concentrations were similar in WT and *Abcb1a/b*$^{-/-}$ mice. This result suggests that the leakiness of the vasculature in this tumor is too much for P-gp to effectively counter the distribution of docetaxel into the tumor. The ipsilateral brain hemisphere also contained 2- to 3-fold more docetaxel than the contralateral brain, which may be due to more distant leaking of docetaxel into adjacent brain. The finding that the concentration in Mel57 tumors in *Abcb1a/b*$^{-/-}$ mice is only ~40% of the level in Mel57VEGF tumors indicates that the BBB in the Mel57 is still more functional, albeit not completely

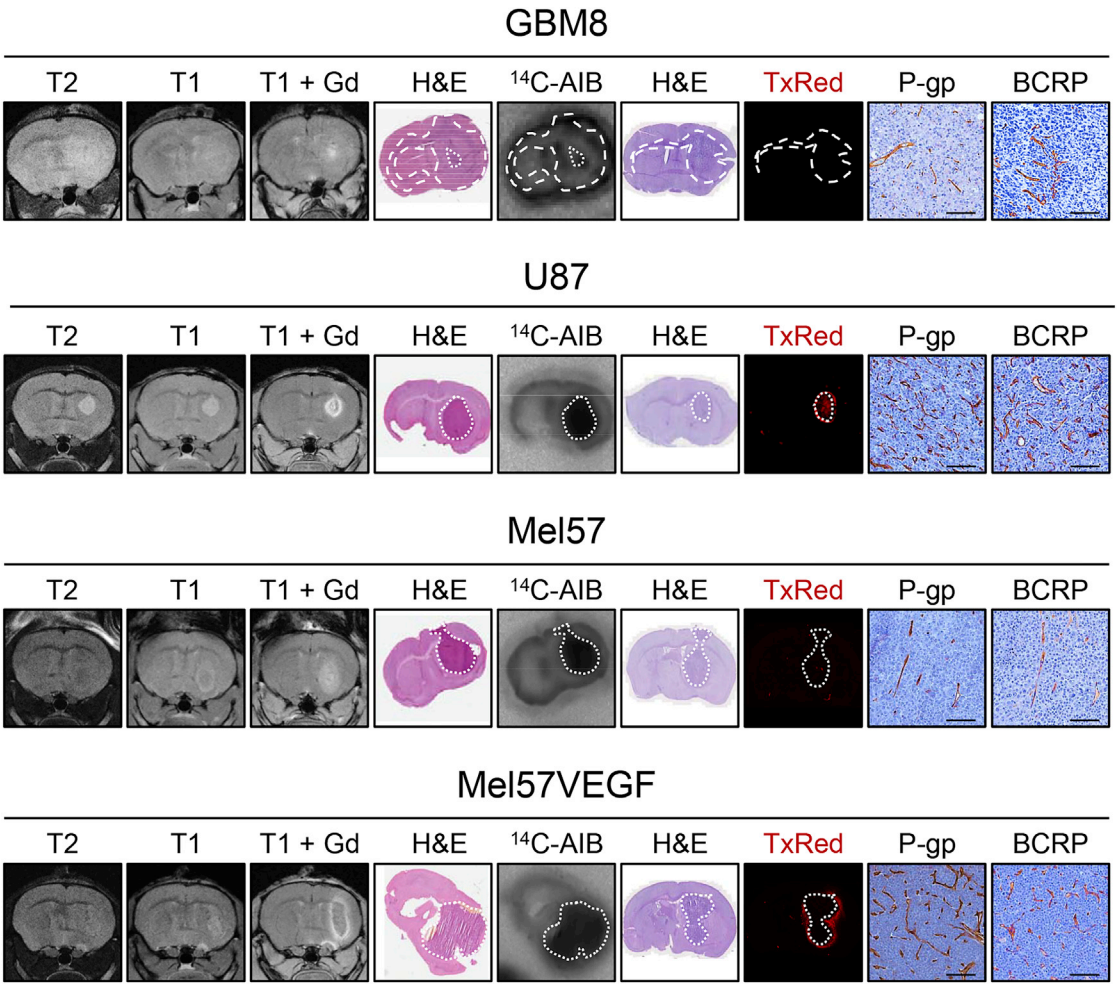

Figure 1. Characterization of the vasculature of intracranial tumor models

The leakiness of the vasculature of intracranial GBM8, U87, Mel57, and Mel57VEGF tumors was assessed by T2-weighted, T1-weighted pre-contrast and T1-weighted post-gadolinium (Gd) contrast magnetic resonance imaging, by autoradiography following intravenous (i.v.) administration of ^{14}C-aminoisobutyrate (AIB) and by fluorescence microscopy following i.v. Texas Red (TxRed). Histochemical hematoxylin and eosin (H&E) staining was used as a reference for tumor location. P-glycoprotein (P-gp) and breast cancer resistance protein (BCRP) expression was demonstrated by immunohistochemistry. All of the microscopy images are representative of n = 5–13 animals. Scale bars, 100 μm.

See also Figures S1 and S2.

tight. The leaky U87 tumors also accumulate 10-fold more docetaxel than normal brain, which is also further enhanced in *Abcb1a/b*$^{-/-}$ mice, again showing that P-gp can reduce the entry of drugs even when vessels are leaky.

A leaky BBB can still protect brain tumors and reduce the efficacy of therapeutics

We used tumor cells expressing luciferase to allow non-invasive longitudinal bioluminescence imaging as a readout of tumor growth for this study. Treatment began ~10–14 days after tumor cell injection. When we challenged Mel57 tumors with paclitaxel or docetaxel, the tumors did not show any response to the treatment, even in *Abcb1a/b*$^{-/-}$ mice (Figures 3A and 3B). Apparently the ~2.5-fold higher docetaxel accumulation in the tumors in *Abcb1a/b*$^{-/-}$ mice was still insufficient to elicit a therapeutic effect. When Mel57VEGF tumors were treated with docetaxel, a robust response was observed, which was similar in WT and *Abcb1a/b*$^{-/-}$ mice (Figure 3C). This is in line with the finding of a similar docetaxel distribution in the tumors grafted in both strains, which was also more than 2-fold higher than in Mel57 tumors (Figure 2). Further evidence that the poor response of intracranial Mel57 tumors is due to protection by the BBB comes from the finding that Mel57 tumors are very responsive to docetaxel when placed under the renal subcapsule (Figure 3D).

GBM8 tumors do not respond to docetaxel treatment, even not in *Abcb1a/b;Abcg2*$^{-/-}$ mice, which is in line with the finding that the accumulation of docetaxel is very low in these tumors (Figures 2 and 4A). Similar results were obtained with the rat-derived glioma model RG2, which we initially used before switching to GBM8 as a more relevant human GBM model. Despite the evidence of some leakiness as observed by fluorescent dyes and AIB, docetaxel

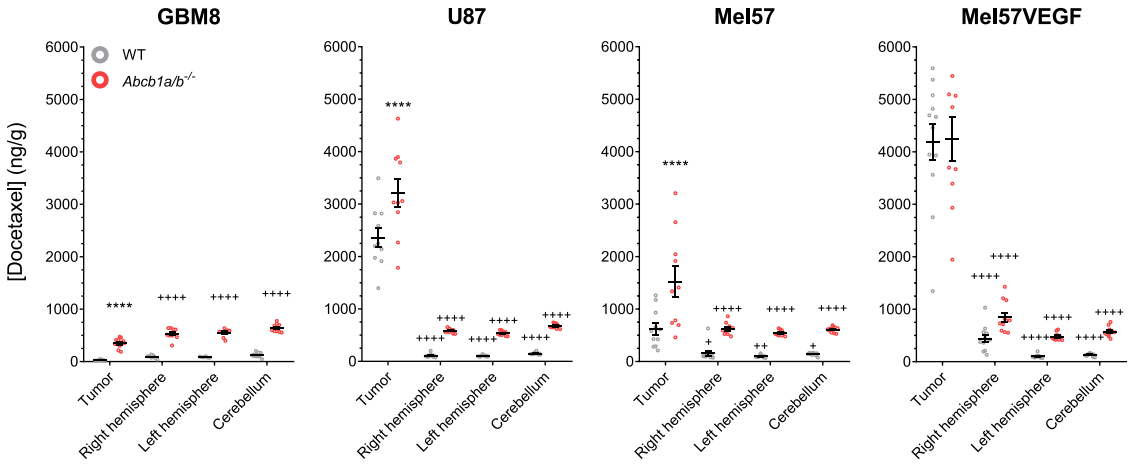

Figure 2. Docetaxel distribution in brain tumors

The docetaxel concentration was lower in Mel57, U87, and GBM8 tumors of wild-type (WT) mice compared to *Abcb1a/b*$^{-/-}$ mice, but considerably higher than in surrounding normal tissues (right hemisphere, left hemisphere, and cerebellum) in all tumors but GBM8. Tissues were harvested at 4 h after 30 mg/kg i.v. docetaxel. Data are represented as means ± SEs (n = 9–12); ****p < 0.0001, for tumor compared to WT; $^{+}$p < 0.05, $^{++++}$p < 0.0001 for normal brain compared to tumor in the same genotype. $^{++}$p < 0.01.

did not demonstrate efficacy against intracranial lesions, whereas it was efficacious against subcutaneous RG2 (Figure S3). In contrast, we observed a response in WT mice when we treated U87 tumors with docetaxel or paclitaxel, which is in line with the finding that these tumors are very leaky (Figures 1, 2,4B, and 4C). Notably, however, despite the fact that U87 tumors have very leaky vessels, the response observed in tumors in *Abcb1a/b*$^{-/-}$ mice was much more profound. This finding demonstrates that the activity of P-gp in otherwise leaky vessels can diminish the efficacy of a drug.

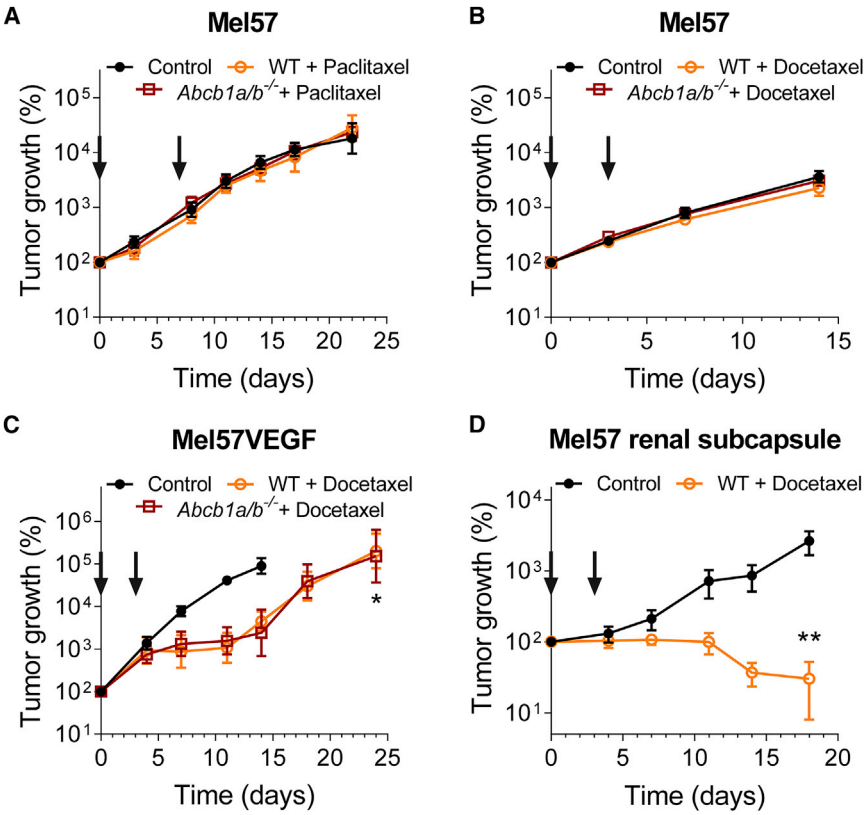

Figure 3. BBB permeability affects the efficacy of treatment against intracranial Mel57 tumors

(A) Efficacy of paclitaxel against intracranial Mel57 tumors grafted in WT or *Abcb1a/b*$^{-/-}$ mice. Data are represented as means ± SEs (n ≥ 6).

(B) Efficacy of docetaxel against intracranial Mel57 tumors grafted in WT or *Abcb1a/b*$^{-/-}$ mice. Data are represented as means ± SEs (n ≥ 8).

(C) Efficacy of docetaxel against intracranial Mel57VEGF tumors grafted in WT or *Abcb1a/b*$^{-/-}$ mice. Data are represented as means ± SEs (n ≥ 7); *p < 0.05.

(D) Efficacy of docetaxel against Mel57 tumors grafted in the renal subcapsule of WT mice. Data are represented as means ± SEs (n ≥ 5); **p < 0.01.

In all of the panels, arrows indicate the days of taxane administration.

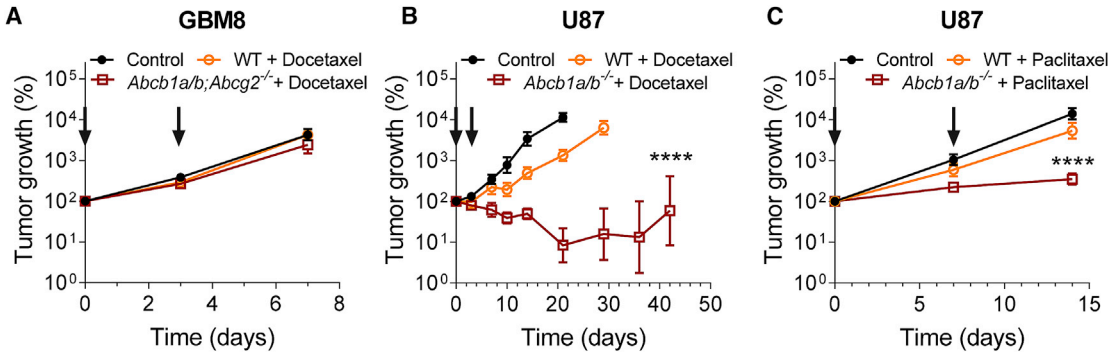

Figure 4. BBB permeability affects the efficacy of treatment against intracranial GBM tumors

(A) Efficacy of docetaxel against intracranial GBM8 tumors grafted in WT or *Abcb1a/b;Abcg2*$^{-/-}$ mice. Data are represented as means ± SEs ($n \geq 6$).

(B) Efficacy of docetaxel against intracranial U87 tumors grafted in WT or *Abcb1a/b*$^{-/-}$ mice. Data are represented as means ± SEs ($n \geq 6$); ****$p < 0.0001$.

(C) Efficacy of paclitaxel against intracranial U87 tumors grafted in WT or *Abcb1a/b*$^{-/-}$ mice. Data are represented as means ± SEs ($n \geq 7$); ****$p < 0.0001$.

In all of the panels, arrows indicate the days of taxane administration.

See also Figure S3.

DISCUSSION

By using our series of orthotopic brain tumor models engrafted into paired sets of P-gp-deficient versus P-gp-proficient nude mice, we show that intracranial tumors that preserve the integrity of the BBB are very well protected against treatment with taxanes, even when P-gp is absent. Intracranial tumors that have leakier BBB properties and are thus more accessible can be more responsive to chemotherapy. Importantly, however, the accumulation of docetaxel in tumors that have leaky blood vessels is significantly higher in *Abcb1a/b*$^{-/-}$ mice compared to WT mice. Moreover, this also translates into better efficacy. This result indicates that drug efflux transporters expressed in tumor vessels may still compromise chemotherapy efficacy, even when tumor blood vessels are leaky. Thus, leakiness of the BBB as determined by MRI does not imply unimpeded access of drugs into brain tumor lesions.

In previous studies on GBM, we have tested more clinically relevant drugs (temozolomide)[20] or experimental drugs (veliparib, phosphatidylinositol 3-kinase [PI3K] inhibitors).[21,22] In some of these studies, we also showed that brain tumors with an (almost) intact barrier respond better to substrate drugs when the transporters are absent. In the present study, we aimed to examine the mechanistic impact of drug transporters in lesions that harbor a leaky barrier, as found in the core regions of GBM. For this purpose, we used docetaxel as a model substrate drug to which tumor cells are generally sensitive and not a drug that requires a specific target.

We designed this study in such a way that it allowed us to establish the impact of BBB integrity and the role of P-gp in blood vessels on drug distribution and antitumor efficacy. We characterized the integrity of tumor blood vessels in a range of brain tumor models and used paired cohorts of nude mice strains that were deficient or proficient for P-gp. We have used docetaxel because it is a substrate of P-gp, but the effect on the plasma clearance by P-gp is minimal, as elimination of docetaxel occurs mainly through CYP450-mediated metabolic degradation.[19,23]

Earlier studies also investigated taxane drugs in brain tumors. Fellner et al.[24]previously showed that the efficacy of paclitaxel against an experimental U118MG brain tumor model was improved when given in combination with the P-gp inhibitor valspodar. They also tested U87 with paclitaxel and valspodar but only at a dose of 4 mg/kg, which was too low for a response. Results by Gallo et al.,[25] who analyzed the distribution of paclitaxel in intracranially grafted B16 melanoma —originating from a C57BL/6 mouse— into WT and *Abcb1a/b*$^{-/-}$ FVB mice, suggested that P-gp limited drug entry in these tumors, although the difference in that study was not significant. The leakiness of these non-syngeneic tumors was not assessed and also the impact on efficacy was not tested. Adkins et al.[26] used rhodamine 123 as a model substrate and showed that the distribution was not increased in leaky breast cancer brain metastases, whereas Goutal et al.[27] demonstrated that focused ultrasound disruption of the BBB of non-tumor-bearing animals did not enhance the brain distribution of erlotinib.

The presence of P-gp and other ABC transporters in the tumor vessels of GBM is well documented, although there is no consensus on the expression changes compared to healthy brain vessels. On the one hand, as determined by immunohistochemistry, blood vessels of primary brain tumors generally stain with similar or sometimes even higher intensities for P-gp and BCRP compared to vessels in normal brain tissue,[28–30] whereas the expression in vessels of metastatic lesions is more diverse.[31–33] Notably, immunohistochemistry provides data on the location of the protein, but the quantitation is less robust. On the other hand, two recent studies using quantitative proteomics on homogenates of isolated microvessels and single-cell RNA sequencing (RNA-seq) reported lower levels of transporter proteins and transcripts in GBM compared to normal brain tissue.[34,35] Proteomics is more quantitative, but it lacks information on spatial distribution and is very much dependent on the vessel content in the homogenate. Moreover, the surgical specimens in both studies are likely to contain more material from the central part of the tumor than from the invasive areas. Taken together, even though their expression level may be

different compared to healthy vessels, the presence of P-gp and BCRP in tumor vessels is well established. It was therefore postulated that drug efflux transporters could still compromise the distribution and efficacy of chemotherapy. Our results demonstrate that this is indeed the case. All of our intracranial tumor models, whether of glial or other origin, expressed both P-gp and BCRP in the tumor vasculature (Figure 1). Of note, tumor cells can also express these drug efflux transporters, and this may form an additional hurdle to effective therapy.[21,36]

It is well established that astrocyte-endothelial cell interactions are crucial for the formation and maintenance of the BBB properties, including the expression of ABC transporters.[6] The finding of ABC transporter expression in non-glial tumors therefore suggests that these tumors grow at least in part via co-option of the preexisting vasculature. Invasion of the brain by GBM cells may occur via various routes, including the perivascular space.[37] Intriguingly, Watkins et al.[38] showed that focal breaches of the BBB may already occur when single invading tumor cells displace the astrocytic endfeet from the endothelial cells. This would imply also that invasive regions of GBM would be less protected by the BBB. However, these results were recently challenged by Pacioni et al.[39] using GSC lines cultured in neurobasal medium instead of serum-cultured GBM lines. These latter results are in line with the unperturbed BBB in our GBM8 model. Obviously, most of the vessels in our models are surrounded by tumor cells and will have less connection with astrocytes; however, this does not annul the expression of ABC transporters.

Patient-derived neurobasal cultured glioma stem-like cells, such as the GBM8 model, much better resemble GBM in human patients than the serum-cultured cell lines such as U87.[40] When the topic of this research would have been to demonstrate the potential usefulness of a given compound for the treatment of GBM, we would certainly not rely on U87 as the test model. U87 is, however, very useful for demonstrating that lesions with leaky vessels can still be protected by ABC transporters in endothelial cells. In our previous work testing experimental agents against GBM, (e.g., in our work on the invasion of GBM),[41] we used more advanced GBM models, including transgenic mouse models and neurobasal-cultured human glioma stem-like cells of different GBM subtypes. Unfortunately, we were not able to use these neurobasal-cultured human GBM models for this work, since they have a very low tumor take in nude mice. Crucial to this study is the availability of a set of ABC transporter-deficient and -proficient recipient mouse strains, and NOD/SCID/IL2Rγ KO mice or NOD/SCID lacking *Abcb1* and/or *Abcg2* are not available.

Interestingly, even tumor vessels in non-glial Mel57VEGF tumors stained intensely for P-gp and BCRP, although the transporters were no longer able to protect the tumor. It has been shown that exposure to ectopic VEGF decreased P-gp functionality in isolated capillaries but did not decrease P-gp expression. Moreover, intracerebroventricular VEGF injection increased the brain distribution of morphine and verapamil, but not of sucrose.[42] Although these results suggest that VEGF can elicit a direct effect on P-gp functionality, disruption of the barrier by VEGF in tumors is a more plausible explanation for the profound distribution of docetaxel in the Mel57-VEGF model. Opening of the BBB by VEGF-producing tumor cells was also found to improve the efficacy of the MDM2 inhibitor SAR405838.[43]

Disruption of the BBB in tumors by VEGF is more likely to occur when lesions become bigger and more hypoxic. Notably, however, although large and lethal for mice, the actual size of the tumor lesions in the mouse brain is very small and likely reflects the size of asymptomatic lesions in patients that may be hard to visualize by MRI. The absence of P-gp and BCRP in blood vessels of surgical samples of brain metastases may be due to the fact that these tumors will be larger and that expression has been lost during their progression from micro-metastasis to clinically overt lesions. Clinical responses in patients with brain metastases occur.[44] In line with this, Fine et al.,[45] who have studied the distribution of paclitaxel in primary and metastatic brain tumors in patients, reported that a higher drug accumulation of paclitaxel was found in metastatic tumors relative to primary brain tumors. Nevertheless, the usefulness of systemic chemotherapy for brain metastases remains controversial.[46,47]

Although the literature suggests that disruption of the BBB provides better access of compounds to brain tumors, our results show that the entry and, consequently, efficacy of substrate drugs may still be limited by drug efflux transporters. Concordant with paclitaxel and docetaxel, other small molecules will be subjected to the same principles. Temozolomide is a relatively BBB-penetrable drug and is able to achieve therapeutic levels in GBM, although we recently showed that even the distribution and efficacy of temozolomide is impeded by drug efflux transporters.[20] Because temozolomide is quite BBB penetrable, the gain in brain distribution in the absence of P-gp and BCRP was small. However, many of the novel targeted agents that have shown profound responses in patients with extracranial malignancies are excellent substrates for P-gp and/or BCRP and are efficiently extruded from the brain.[48] Consequently, it will clearly be advantageous for the treatment of intracranial tumors to focus on those candidate drugs that readily cross the BBB. Concomitant use of potent inhibitors of the efflux transporters such as elacridar may be an alternative when BBB-penetrable candidates are not available.

In conclusion, leakiness of the BBB does not guarantee good accessibility of drugs to brain tumors—in particular, when present as small lesions. Although therapeutics may be able to exert a response against brain tumors, the full potential of the therapy may still be attenuated by drug efflux pumps in the tumor vessels.

Limitations of study

This study was conducted in mice, which differ from humans in several aspects. The size of a brain lesion that is end-stage disease in a mouse is still very small for humans. The time to develop these lesions is probably also shorter in mice, and the expression of the ABC transporters in the vessels of larger brain lesions in humans may therefore be different. Thus, our work may be more applicable to smaller lesions. Furthermore, by using docetaxel, we focused on the role of P-gp, whereas BCRP may be more important than P-gp at the human BBB since it is more abundantly expressed. Lastly, we needed to conduct paired studies in brain tumor-bearing ABC transporter-proficient and -deficient animals. Since only thymus-less (nude) mice were

available as suitable recipients of human tissues, we were limited in the choice of human GSC lines to GBM8. Most GSC lines require more immunocompromised NOD/SCID or NOD/SCID/IL2Rγ null mice, but these are not available as ABC transporter-deficient mice.

STAR★METHODS

Detailed methods are provided in the online version of this paper and include the following:

- KEY RESOURCES TABLE
- RESOURCE AVAILABILITY
  - Lead contact
  - Materials availability
  - Data and code availability
- EXPERIMENTAL MODEL AND SUBJECT DETAILS
  - Cells
  - Animals
  - Experimental *in vivo* tumor models
- METHOD DETAILS
  - Drugs and compounds
  - Magnetic resonance imaging
  - Blood-brain barrier permeability analysis
  - Histology and immunohistochemistry
  - Drug concentration measurements
  - *In vivo* efficacy studies
- QUANTIFICATION AND STATISTICAL ANALYSIS

SUPPLEMENTAL INFORMATION

Supplemental Information can be found online at https://doi.org/10.1016/j.xcrm.2020.100184.

ACKNOWLEDGMENTS

This work was financially supported by a research grant of the Dutch Cancer Society (KWF) to O.v.T. The authors thank Piotr Waranecki and Hans Meel for conducting the STR analyses. The authors thank Marjolijn Mertz, Amalie Dick, and Lenny Brocks from the NKI BioImaging Facility for their assistance with image processing and analysis.

AUTHOR CONTRIBUTIONS

Design & Supervision, J.H.B. and O.v.T. Design & Execution of the Experiments and Interpretation of the Data, M.C.d.G., E.M.K., L.C.M.B., C.H.Ç., T.B., and O.v.T. Manuscript Writing, M.C.d.G. and O.v.T., with input from all of the other authors.

DECLARATION OF INTERESTS

The authors declare no competing interests.

Received: March 25, 2020
Revised: July 21, 2020
Accepted: December 16, 2020
Published: January 19, 2021

REFERENCES

1. Stupp, R., Mason, W.P., van den Bent, M.J., Weller, M., Fisher, B., Taphoorn, M.J., Belanger, K., Brandes, A.A., Marosi, C., Bogdahn, U., et al.; European Organisation for Research and Treatment of Cancer Brain Tumor and Radiotherapy Groups; National Cancer Institute of Canada Clinical Trials Group (2005). Radiotherapy plus concomitant and adjuvant temozolomide for glioblastoma. N. Engl. J. Med. *352*, 987–996.
2. Sarkaria, J.N., Hu, L.S., Parney, I.F., Pafundi, D.H., Brinkmann, D.H., Laack, N.N., Giannini, C., Burns, T.C., Kizilbash, S.H., Laramy, J.K., et al. (2018). Is the blood-brain barrier really disrupted in all glioblastomas? A critical assessment of existing clinical data. Neuro Oncol. *20*, 184–191.
3. Durmus, S., Hendrikx, J.J., and Schinkel, A.H. (2015). Apical ABC transporters and cancer chemotherapeutic drug disposition. Adv. Cancer Res. *125*, 1–41.
4. van Tellingen, O., Yetkin-Arik, B., de Gooijer, M.C., Wesseling, P., Wurdinger, T., and de Vries, H.E. (2015). Overcoming the blood-brain tumor barrier for effective glioblastoma treatment. Drug Resist. Updat. *19*, 1–12.
5. Abbott, N.J., Patabendige, A.A., Dolman, D.E., Yusof, S.R., and Begley, D.J. (2010). Structure and function of the blood-brain barrier. Neurobiol. Dis. *37*, 13–25.
6. Abbott, N.J., Rönnbäck, L., and Hansson, E. (2006). Astrocyte-endothelial interactions at the blood-brain barrier. Nat. Rev. Neurosci. *7*, 41–53.
7. Lin, F., Marchetti, S., Pluim, D., Iusuf, D., Mazzanti, R., Schellens, J.H., Beijnen, J.H., and van Tellingen, O. (2013). Abcc4 together with abcb1 and abcg2 form a robust cooperative drug efflux system that restricts the brain entry of camptothecin analogues. Clin. Cancer Res. *19*, 2084–2095.
8. Nduom, E.K., Yang, C., Merrill, M.J., Zhuang, Z., and Lonser, R.R. (2013). Characterization of the blood-brain barrier of metastatic and primary malignant neoplasms. J. Neurosurg. *119*, 427–433.
9. Upadhyay, N., and Waldman, A.D. (2011). Conventional MRI evaluation of gliomas. Br. J. Radiol. *84*, S107–S111.
10. Lockman, P.R., Mittapalli, R.K., Taskar, K.S., Rudraraju, V., Gril, B., Bohn, K.A., Adkins, C.E., Roberts, A., Thorsheim, H.R., Gaasch, J.A., et al. (2010). Heterogeneous blood-tumor barrier permeability determines drug efficacy in experimental brain metastases of breast cancer. Clin. Cancer Res. *16*, 5664–5678.
11. Parrish, K.E., Pokorny, J., Mittapalli, R.K., Bakken, K., Sarkaria, J.N., and Elmquist, W.F. (2015). Efflux transporters at the blood-brain barrier limit delivery and efficacy of cyclin-dependent kinase 4/6 inhibitor palbociclib (PD-0332991) in an orthotopic brain tumor model. J. Pharmacol. Exp. Ther. *355*, 264–271.
12. Pokorny, J.L., Calligaris, D., Gupta, S.K., Iyekegbe, D.O., Jr., Mueller, D., Bakken, K.K., Carlson, B.L., Schroeder, M.A., Evans, D.L., Lou, Z., et al. (2015). The Efficacy of the Wee1 Inhibitor MK-1775 Combined with Temozolomide Is Limited by Heterogeneous Distribution across the Blood-Brain Barrier in Glioblastoma. Clin. Cancer Res. *21*, 1916–1924.
13. Huizing, M.T., Misser, V.H., Pieters, R.C., ten Bokkel Huinink, W.W., Veenhof, C.H., Vermorken, J.B., Pinedo, H.M., and Beijnen, J.H. (1995). Taxanes: a new class of antitumor agents. Cancer Invest. *13*, 381–404.
14. Prados, M.D., Schold, S.C., Spence, A.M., Berger, M.S., McAllister, L.D., Mehta, M.P., Gilbert, M.R., Fulton, D., Kuhn, J., Lamborn, K., et al. (1996). Phase II study of paclitaxel in patients with recurrent malignant glioma. J. Clin. Oncol. *14*, 2316–2321.
15. Chamberlain, M.C., and Kormanik, P. (1999). Salvage chemotherapy with taxol for recurrent anaplastic astrocytomas. J. Neurooncol. *43*, 71–78.
16. Cahan, M.A., Walter, K.A., Colvin, O.M., and Brem, H. (1994). Cytotoxicity of taxol in vitro against human and rat malignant brain tumors. Cancer Chemother. Pharmacol. *33*, 441–444.
17. Terzis, A.J., Thorsen, F., Heese, O., Visted, T., Bjerkvig, R., Dahl, O., Arnold, H., and Gundersen, G. (1997). Proliferation, migration and invasion of human glioma cells exposed to paclitaxel (Taxol) in vitro. Br. J. Cancer *75*, 1744–1752.
18. Kemper, E.M., van Zandbergen, A.E., Cleypool, C., Mos, H.A., Boogerd, W., Beijnen, J.H., and van Tellingen, O. (2003). Increased penetration of

paclitaxel into the brain by inhibition of P-glycoprotein. Clin. Cancer Res. *9*, 2849–2855.

19. Kemper, E.M., Verheij, M., Boogerd, W., Beijnen, J.H., and van Tellingen, O. (2004). Improved penetration of docetaxel into the brain by co-administration of inhibitors of P-glycoprotein. Eur. J. Cancer *40*, 1269–1274.
20. de Gooijer, M.C., de Vries, N.A., Buckle, T., Buil, L.C.M., Beijnen, J.H., Boogerd, W., and van Tellingen, O. (2018). Improved Brain Penetration and Antitumor Efficacy of Temozolomide by Inhibition of ABCB1 and ABCG2. Neoplasia *20*, 710–720.
21. Lin, F., de Gooijer, M.C., Roig, E.M., Buil, L.C., Christner, S.M., Beumer, J.H., Würdinger, T., Beijnen, J.H., and van Tellingen, O. (2014). ABCB1, ABCG2, and PTEN determine the response of glioblastoma to temozolomide and ABT-888 therapy. Clin. Cancer Res. *20*, 2703–2713.
22. Lin, F., de Gooijer, M.C., Hanekamp, D., Chandrasekaran, G., Buil, L.C., Thota, N., Sparidans, R.W., Beijnen, J.H., Würdinger, T., and van Tellingen, O. (2017). PI3K-mTOR Pathway Inhibition Exhibits Efficacy Against High-grade Glioma in Clinically Relevant Mouse Models. Clin. Cancer Res. *23*, 1286–1298.
23. van Waterschoot, R.A., Lagas, J.S., Wagenaar, E., van der Kruijssen, C.M., van Herwaarden, A.E., Song, J.Y., Rooswinkel, R.W., van Tellingen, O., Rosing, H., Beijnen, J.H., and Schinkel, A.H. (2009). Absence of both cytochrome P450 3A and P-glycoprotein dramatically increases docetaxel oral bioavailability and risk of intestinal toxicity. Cancer Res. *69*, 8996–9002.
24. Fellner, S., Bauer, B., Miller, D.S., Schaffrik, M., Fankhänel, M., Spruss, T., Bernhardt, G., Graeff, C., Färber, L., Gschaidmeier, H., et al. (2002). Transport of paclitaxel (Taxol) across the blood-brain barrier in vitro and in vivo. J. Clin. Invest. *110*, 1309–1318.
25. Gallo, J.M., Li, S., Guo, P., Reed, K., and Ma, J. (2003). The effect of P-glycoprotein on paclitaxel brain and brain tumor distribution in mice. Cancer Res. *63*, 5114–5117.
26. Adkins, C.E., Mittapalli, R.K., Manda, V.K., Nounou, M.I., Mohammad, A.S., Terrell, T.B., Bohn, K.A., Yasemin, C., Grothe, T.R., Lockman, J.A., and Lockman, P.R. (2013). P-glycoprotein mediated efflux limits substrate and drug uptake in a preclinical brain metastases of breast cancer model. Front. Pharmacol. *4*, 136.
27. Goutal, S., Gerstenmayer, M., Auvity, S., Caillé, F., Mériaux, S., Buvat, I., Larrat, B., and Tournier, N. (2018). Physical blood-brain barrier disruption induced by focused ultrasound does not overcome the transporter-mediated efflux of erlotinib. J. Control. Release *292*, 210–220.
28. Demeule, M., Shedid, D., Beaulieu, E., Del Maestro, R.F., Moghrabi, A., Ghosn, P.B., Moumdjian, R., Berthelet, F., and Béliveau, R. (2001). Expression of multidrug-resistance P-glycoprotein (MDR1) in human brain tumors. Int. J. Cancer *93*, 62–66.
29. Fattori, S., Becherini, F., Cianfriglia, M., Parenti, G., Romanini, A., and Castagna, M. (2007). Human brain tumors: multidrug-resistance P-glycoprotein expression in tumor cells and intratumoral capillary endothelial cells. Virchows Arch. *451*, 81–87.
30. Emery, I.F., Gopalan, A., Wood, S., Chow, K.H., Battelli, C., George, J., Blaszyk, H., Florman, J., and Yun, K. (2017). Expression and function of ABCG2 and XIAP in glioblastomas. J. Neurooncol. *133*, 47–57.
31. Tóth, K., Vaughan, M.M., Peress, N.S., Slocum, H.K., and Rustum, Y.M. (1996). MDR1 P-glycoprotein is expressed by endothelial cells of newly formed capillaries in human gliomas but is not expressed in the neovasculature of other primary tumors. Am. J. Pathol. *149*, 853–858.
32. Yonemori, K., Tsuta, K., Ono, M., Shimizu, C., Hirakawa, A., Hasegawa, T., Hatanaka, Y., Narita, Y., Shibui, S., and Fujiwara, Y. (2010). Disruption of the blood brain barrier by brain metastases of triple-negative and basal-type breast cancer but not HER2/neu-positive breast cancer. Cancer *116*, 302–308.
33. Richtig, E., Asslaber, M., Partl, R., Avian, A., Berghold, A., Kapp, K., Preusser, M., Becker, J.C., and Curiel-Lewandrowski, C. (2016). Lack of P-glycoprotein expression in melanoma brain metastases of different melanoma types. Clin. Neuropathol. *35*, 89–92.
34. Bao, X., Wu, J., Xie, Y., Kim, S., Michelhaugh, S., Jiang, J., Mittal, S., Sanai, N., and Li, J. (2020). Protein Expression and Functional Relevance of Efflux and Uptake Drug Transporters at the Blood-Brain Barrier of Human Brain and Glioblastoma. Clin. Pharmacol. Ther. *107*, 1116–1127.
35. Dusart, P., Hallström, B.M., Renné, T., Odeberg, J., Uhlén, M., and Butler, L.M. (2019). A Systems-Based Map of Human Brain Cell-Type Enriched Genes and Malignancy-Associated Endothelial Changes. Cell Rep. *29*, 1690–1706.e4.
36. Agarwal, S., Mittapalli, R.K., Zellmer, D.M., Gallardo, J.L., Donelson, R., Seiler, C., Decker, S.A., Santacruz, K.S., Pokorny, J.L., Sarkaria, J.N., et al. (2012). Active efflux of Dasatinib from the brain limits efficacy against murine glioblastoma: broad implications for the clinical use of molecularly targeted agents. Mol. Cancer Ther. *11*, 2183–2192.
37. de Gooijer, M.C., Guillén Navarro, M., Bernards, R., Wurdinger, T., and van Tellingen, O. (2018). An Experimenter's Guide to Glioblastoma Invasion Pathways. Trends Mol. Med. *24*, 763–780.
38. Watkins, S., Robel, S., Kimbrough, I.F., Robert, S.M., Ellis-Davies, G., and Sontheimer, H. (2014). Disruption of astrocyte-vascular coupling and the blood-brain barrier by invading glioma cells. Nat. Commun. *5*, 4196.
39. Pacioni, S., D'Alessandris, Q.G., Buccarelli, M., Boe, A., Martini, M., Larocca, L.M., Bolasco, G., Ricci-Vitiani, L., Falchetti, M.L., and Pallini, R. (2019). Brain Invasion along Perivascular Spaces by Glioma Cells: Relationship with Blood-Brain Barrier. Cancers (Basel) *12*, 18.
40. Lee, J., Kotliarova, S., Kotliarov, Y., Li, A., Su, Q., Donin, N.M., Pastorino, S., Purow, B.W., Christopher, N., Zhang, W., et al. (2006). Tumor stem cells derived from glioblastomas cultured in bFGF and EGF more closely mirror the phenotype and genotype of primary tumors than do serum-cultured cell lines. Cancer Cell *9*, 391–403.
41. Pencheva, N., de Gooijer, M.C., Vis, D.J., Wessels, L.F.A., Würdinger, T., van Tellingen, O., and Bernards, R. (2017). Identification of a Druggable Pathway Controlling Glioblastoma Invasiveness. Cell Rep. *20*, 48–60.
42. Hawkins, B.T., Sykes, D.B., and Miller, D.S. (2010). Rapid, reversible modulation of blood-brain barrier P-glycoprotein transport activity by vascular endothelial growth factor. J. Neurosci. *30*, 1417–1425.
43. Kim, M., Ma, D.J., Calligaris, D., Zhang, S., Feathers, R.W., Vaubel, R.A., Meaux, I., Mladek, A.C., Parrish, K.E., Jin, F., et al. (2018). Efficacy of the MDM2 Inhibitor SAR405838 in Glioblastoma Is Limited by Poor Distribution Across the Blood-Brain Barrier. Mol. Cancer Ther. *17*, 1893–1901.
44. Davies, M.A., Saiag, P., Robert, C., Grob, J.-J., Flaherty, K.T., Arance, A., Chiarion-Sileni, V., Thomas, L., Lesimple, T., Mortier, L., et al. (2017). Dabrafenib plus trametinib in patients with $BRAF^{V600}$-mutant melanoma brain metastases (COMBI-MB): a multicentre, multicohort, open-label, phase 2 trial. Lancet Oncol. *18*, 863–873.
45. Fine, R.L., Chen, J., Balmaceda, C., Bruce, J.N., Huang, M., Desai, M., Sisti, M.B., McKhann, G.M., Goodman, R.R., Bertino, J.S., Jr., et al. (2006). Randomized study of paclitaxel and tamoxifen deposition into human brain tumors: implications for the treatment of metastatic brain tumors. Clin. Cancer Res. *12*, 5770–5776.
46. Fortin, D. (2012). The blood-brain barrier: its influence in the treatment of brain tumors metastases. Curr. Cancer Drug Targets *12*, 247–259.
47. Mehta, M.P., Paleologos, N.A., Mikkelsen, T., Robinson, P.D., Ammirati, M., Andrews, D.W., Asher, A.L., Burri, S.H., Cobbs, C.S., Gaspar, L.E., et al. (2010). The role of chemotherapy in the management of newly diagnosed brain metastases: a systematic review and evidence-based clinical practice guideline. J. Neurooncol. *96*, 71–83.
48. Kim, M., Kizilbash, S.H., Laramy, J.K., Gampa, G., Parrish, K.E., Sarkaria, J.N., and Elmquist, W.F. (2018). Barriers to Effective Drug Treatment for Brain Metastases: A Multifactorial Problem in the Delivery of Precision Medicine. Pharm. Res. *35*, 177.
49. Xie, Y., Bergström, T., Jiang, Y., Johansson, P., Marinescu, V.D., Lindberg, N., Segerman, A., Wicher, G., Niklasson, M., Baskaran, S., et al. (2015).

The Human Glioblastoma Cell Culture Resource: Validated Cell Models Representing All Molecular Subtypes. EBioMedicine *2*, 1351–1363.

50. Kemper, E.M., Leenders, W., Küsters, B., Lyons, S., Buckle, T., Heerschap, A., Boogerd, W., Beijnen, J.H., and van Tellingen, O. (2006). Development of luciferase tagged brain tumour models in mice for chemotherapy intervention studies. Eur. J. Cancer *42*, 3294–3303.

51. Singh, R.K., Bucana, C.D., Gutman, M., Fan, D., Wilson, M.R., and Fidler, I.J. (1994). Organ site-dependent expression of basic fibroblast growth factor in human renal cell carcinoma cells. Am. J. Pathol. *145*, 365–374.

52. Schindelin, J., Arganda-Carreras, I., Frise, E., Kaynig, V., Longair, M., Pietzsch, T., Preibisch, S., Rueden, C., Saalfeld, S., Schmid, B., et al. (2012). Fiji: an open-source platform for biological-image analysis. Nat. Methods *9*, 676–682.

53. Stokvis, E., Ouwehand, M., Nan, L.G., Kemper, E.M., van Tellingen, O., Rosing, H., and Beijnen, J.H. (2004). A simple and sensitive assay for the quantitative analysis of paclitaxel in human and mouse plasma and brain tumor tissue using coupled liquid chromatography and tandem mass spectrometry. J. Mass Spectrom. *39*, 1506–1512.

STAR★METHODS

KEY RESOURCES TABLE

REAGENT or RESOURCE	SOURCE	IDENTIFIER
Antibodies		
Rabbit monoclonal antibody MDR1/ABCB1 (E1Y7S)	Cell Signaling	#13978; RRID:AB_2798357
Rat monoclonal antibody BCRP/ABCG2 (BXP-53)	Abcam	Ab24115; RRID:AB_447879
Chemicals, peptides, and recombinant proteins		
^{14}C-aminoisobutyrate (AIB)	Tjaden Biosciences, Burlington, IA, USA	N/A
Dextran, Fluorescein, 3,000 MW Anionic	Invitrogen/ Thermo	D3305
Dextran, Fluorescein, 10,000 MW Anionic	Invitrogen/ Thermo	D1821
Sulforhodamine 101 (TexasRed)	Invitrogen/ Thermo	11570676
Paclitaxel (Taxol©)	Bristol Myers Squibb	N/A
Docetaxel	Hospira, UK	N/A
Temozolomide	Schering Plough	N/A
Neuro-basal medium	Thermo Fisher	10888022
DMEM/F12 Glutamax	Thermo Fisher	10565018
B-27 Supplement (50x), minus vitamin A	Thermo Fisher	12587010
Recombinant Human Epidermal Growth Factor (rEGF)	Peprotech	#AF100-15
Recombinant Human Fibroblast Growth Factor (rFGFb)	Peprotech	#100-18B
Minimum essential medium (MEM	Thermo Fisher	31095052
L-glutamine	Thermo Fisher s	25030024
Sodium pyruvate	Thermo Fisher	11360039
Vitamins	Thermo Fisher	11120-037
Penicillin / Streptomycin	Thermo Fisher	15140122
Non-essential amino acids	Thermo Fisher	11140035
Fetal Calf serum	Thermo Fisher	10500064
Gadoterate meglumine (Dotarem®)	Guerbet; Villepinte, France	N/A
D-luciferin	Promega, Madison, WI, USA	E1605
Trypsin-EDTA	Thermo Fisher	25300054
Experimental models: cell lines		
Mel57, Mel57VEGF	Dr W.P. Leenders, (Radboud UMC, Nijmegen, NL)	RRID:CVCL_4454
GBM8	Bakhos Tannous (MGH, Boston, USA)	N/A
U87	ATCC, Manassas, VA, USA	RRID: CVCL_0022
RG2	ATCC, Manassas, VA, USA	RRID: CVCL_3581
Experimental models: organisms/strains		
Mouse: Friends Virus B (FVB) nude	NKI animal facility	N/A
Mouse: Abcb1a/b$^{-/-}$ FVB nude	NKI animal facility	N/A
Mouse: Abcg2$^{-/-}$;Abcb1a/b$^{-/-}$ FVB nude	NKI animal facility	N/A
Software and algorithms		
Living Image 4.5	Perkin Elmer	https://www.perkinelmer.com
Graphpad Prism 7.03	Graphpad	https://www.graphpad.com
Aperio ImageScope v12	Aperio Technologies	https://www.leicabiosystems.com
SPSS v22	SPSS Inc	https://www.ibm.com

(*Continued on next page*)

Continued

REAGENT or RESOURCE	SOURCE	IDENTIFIER
Fiji / ImageJ 1.52n	NIH	https://imagej.nih.gov/ij/
Paravision software (v 6.0.1)	Bruker	https://www.bruker.com
ZEN Blue v3.1	Carl Zeiss	www.zeis.com
HALO v3.1.10076.423	Indica Labs	https://www.indicalab.com

RESOURCE AVAILABILITY

Lead contact

Requests for further information and reagents may be addressed to the corresponding author: Olaf van Tellingen (o.v.tellingen@nki.nl).

Materials availability

Mouse strains can be made available under appropriate materials and treatment agreement. No other unique reagents were generated.

Data and code availability

The data that support the findings of this study are available [Mendeley Data, V1, https://doi.org/10.17632/vkxm4zp7s3.1].

EXPERIMENTAL MODEL AND SUBJECT DETAILS

Cells

The melanoma cell line Mel57 (RRID:CVCL_4454) and its vascular endothelial growth factor (VEGF)-A165 transfected subline Mel57-VEGF were kindly provided by dr. W.P. Leenders (Radboud University Medical Center, Nijmegen, the Netherlands) and the GBM8 cell line expressing firefly luciferase (Fluc) and mCherry by dr. Bakhos Tannous (Massachusetts General Hospital, Boston, MA). The U87 cell line (RRID:CVCL_0022) and RG2 cell line (RRID:CVCL_3581) were obtained from the American Type Culture Collection (ATCC; Manassas, VA). With the exception of the GBM8 glioma stem-like cells, all cell lines were cultured in Minimum Essential Medium, supplemented with 1% L-glutamine, 1% sodium-pyruvate, 1% MEM vitamins, 1% penicillin/streptomycin, 1% non-essential amino acids and 10% fetal calf serum (all from Life Technologies, Carlsbad, CA) and maintained in 5% CO_2 in humidified air at 37°C. GBM8 cells were cultured in 50% Neurobasal medium and 50% DMEM/F12 GlutaMAX supplemented with 2% B-27 without vitamin A (all from Life Technologies) and 10 ng/mL bFGF and EGF (both from PeproTech; London, UK).[49] All serum-cultured cell lines were stably transfected with firefly luciferase and GFP as described previously.[50] All cell lines have been authenticated by STR profiling using the GenePrint 10 system (Promega; Madison, WI) within the last three years (see Table S1) and were cultured mycoplasma-free, as confirmed by PCR. All cell lines were also tested negative for mouse pathogens by Impact I PCR profile (2) (IDEXX, Ludwigsburg, Germany).

Animals

All mice were bred at the Netherlands Cancer Institute and were of Friends Virus B (FVB) strain. Male and female nude mice aged between 8 and 15 weeks were healthy and naive. Wild-type (WT), *Abcb1a/b*$^{-/-}$ and *Abcb1a/b;Abcg2*$^{-/-}$ genotypes were used. Mice were housed in individually ventilated cages using a 12 hours light /12 hours dark cycle. Animals had access to food and water *ad libitum*. Experiments with animals were carried out according to Institutional guidelines, conform the code of practice for animal research in oncology and in line with Dutch and European legislation. All animal experiments were approved by the local Animal Experiments Committee.

Experimental *in vivo* tumor models

Adherent cells (Mel57, Mel57VEGF, U87, RG2) were detached by treatment with trypsin/EDTA (0.05%/0.02%). Trypsin was inactivated by adding complete medium and cells were washed twice with Hanks Balanced Salt Solution (HBSS; Life Technologies). Cells were maintained on ice and used within 6 hours. Neurosphere-cultured GBM8 cells were centrifuged (5 min, 200 g). The pellet was resuspended in trypsin/EDTA (1:15) in saline for 1 min at 37°C and processed to a near single cell suspension by repeated trituration. Experimental intracranial brain tumors were established by intracranial injection of a 2 μL cell suspension containing $1x10^5$ cells (Mel57-Fluc, U87-Fluc and GBM8-Fluc) or $5x10^3$ cells (Mel57VEGF-Fluc and RG2-Fluc) as described previously.[50] To establish extracranial tumor models, $5x10^5$ Mel57-Fluc cells were injected in a volume of 20 μl of HBSS under the renal subcapsule as described previously.[51] A small incision was made in the mouse left flank. The kidney was lifted out of the peritoneum and a 30 g

needle was inserted into the lower pole and advanced until its tip reached just under the renal subcapsule. Subcutaneous RG2-Fluc tumors were established by injection of $5x10^5$ cells suspended in 50 ul of HBBS. Tumor size was measured using calipers and volumes were calculated in mm^3 by the formula: $V = 0.5 \times length \times width^2$.

METHOD DETAILS

Drugs and compounds

Paclitaxel was from Bristol-Myers Squibb (New York, NY). Docetaxel was from Hospira (UK), Temozolomide (Temodal® 100 mg hard capsules) from Schering Plough BV (Utrecht, the Netherlands), ^{14}C-aminoisobutyrate (AIB) from Tjaden Biosciences, (Burlington, IA) and TexasRed (Sulfurodamine 101) and 10kD-Dextran-FITC both from Life Technologies.

Magnetic resonance imaging

Magnetic resonance imaging was done on a BioSpec 70/20 USR (Bruker; Billerica, MA) system using a sequence consisting of T2-weighted, T1-weighted pre-contrast and T1-weighted post-contrast imaging. Gadoterate meglumine (Dotarem®; Guerbet; Villepinte, France) diluted five-fold with saline was used as a contrasting agent and delivered via an intravenous cannula inserted in the tail vein. Mice were anesthetized using isoflurane (Pharmachemie B.V., Haarlem, the Netherlands) delivered via a customized mouse holder, and heart rate and breathing frequency were monitored throughout the entire procedure. Paravision software (v 6.0.1; Bruker) was used for image acquisition and Fiji[52] (v 1.49b) was used for image processing.

Blood-brain barrier permeability analysis

Mice bearing established orthotopic brain tumors were administered 25 μCi of ^{14}C-aminoisobutyrate (AIB) in 100 μl of saline, Sulforhodamine 101 (Texas Red; TxRed; 6 mg/kg) and/or 10kD Dextran–fluorescein (5 mg/kg) and after 30 minutes anesthetized with hypnorm/dormicum and subsequently perfused with saline. The brain was immediately frozen on dry ice in Tissue-Tek® (Sakura Finetek Europe BV; Alphen aan den Rijn, the Netherlands) and kept at −80°C until sectioning. ^{14}C-AIB extravasation was visualized using autoradiography using a FLA-3000 phospho-imager (Fujifilm, Tokyo, Japan), whereas TxRed and 10kD-Dextran-lluorescein were imaged using a Axio Scan.Z1 (Carl Zeiss; Oberkochen, Germany) and subsequently processed and analyzed using ZEN Blue (v3.1; Carl Zeiss) and HALO (v3.1.10076.423; Indica Labs, Albuquerque, NM).

Histology and immunohistochemistry

Tumor-bearing mouse brains were fixed in 4% (v/v) formaldehyde, paraffin embedded and cut into 4 μm coronal sections that were stained with hematoxylin and eosin (H&E), and for P-gp (1:200; 13978; Cell Signaling Technology; Danvers, MA) and BCRP (1:400; ab24115; Abcam; Cambridge, UK). Sections were scanned and processed using an Aperio AT2 system and ImageScope software v12 (both Leica; Wetzlar, Germany).

Drug concentration measurements

Tumor-bearing mice received 33 mg/kg docetaxel i.v. once. Four hours after administration, animals were sacrificed and the brains were collected and divided into four parts: tumor, right (ipsilateral) hemisphere, left (contralateral) hemisphere and cerebellum. Taxane concentrations in brain and brain tumor tissue samples were analyzed by LC–MS/MS as described previously.[53]

In vivo efficacy studies

Paclitaxel was administered i.v. twice at a dose of 20 mg/kg and docetaxel was applied i.v. twice at a dose of 33 mg/kg, as indicated by arrows in each appropriate figure. The drug solutions were prepared with sterile saline to yield final concentrations of 2.0 and 3.3 mg/ml of paclitaxel and docetaxel, respectively and were administered by i.v. bolus injection into the tail vein using 10 μl per gram body weight. Temozolomide was given p.o. at a dose of 100 mg/kg once daily for 5 consecutive days. The content of a temozolomide capsule containing 100 mg of active substance was dissolved in 2 mL ethanol and 18 mL saline to yield a solution of 5.0 mg/mL and was used within 60 minutes after preparation. The control group mice comprised a mix of WT and knockout mice, which received only vehicle.

Bioluminescence images were acquired following i.p. D-luciferin (150 mg/kg; Promega; Madison, WI) using an IVIS 200 or IVIS Spectrum system with Living Image software v4.5 (both PerkinElmer; Waltham, MA). Animals were stratified into treatment groups (WT, *Abcb1a/b*$^{-/-}$ and *Abcb1a/b;Abcg2*$^{-/-}$ mice) and untreated controls (mix of strains) to achieve a similar mean bioluminescence reading within each cohort. The bioluminescence intensity of each individual animal at the day of start of treatment (day 0) was arbitrarily set at 100%. All subsequent measurements were recorded relative to this first measurement and converted to their log-values. Mean ± standard error (SE) values were calculated and plotted in graphs. Mice were weighed daily weighed examined for abnormalities. The mice were humanely sacrificed based on bioluminescence imaging results or when weight loss exceeded 20% of the initial body weight. Following sacrifice, brains were collected in formalin and used to qualitatively assess the tumor size by histology.

QUANTIFICATION AND STATISTICAL ANALYSIS

Statistical calculations were done using the software package SPSS (v22; SPSS Inc; Chicago, IL). *In vivo* tumor growth curves were compared using the General Linear Model repeated-measures procedure. All comparisons of docetaxel concentrations involving more two experimental groups and multiple brain regions were done using two-way analysis of variance (ANOVA) followed by post hoc Bonferroni tests. All group sizes can be found in the appropriate figure legends.